

Combined parametrization of the neutron electric form factor and the $\gamma^* N \rightarrow \Delta(1232)$ quadrupole form factors

G. Ramalho

*Laboratório de Física Teórica e Computacional – LFTC,
Universidade Cruzeiro do Sul, 01506-000, São Paulo, SP, Brazil*

(Dated: December 14, 2024)

Models based on $SU(6)$ symmetry breaking and large N_c limit provide relations between the pion cloud contributions to the $\gamma^* N \rightarrow \Delta(1232)$ quadrupole form factors, electric (G_E) and Coulomb (G_C), and the neutron electric form factor G_{En} , suggesting that those form factors are dominated by the same physical processes. Those relations are improved in order to satisfy a fundamental constraint between the electric and Coulomb quadrupole form factors in the long wavelength limit, when the photon three-momentum vanishes (Siegert's theorem). Inspired by those relations we study alternative parametrizations for the neutron electric form factor. The parameters of the new form are then determined by a combined fit to the G_{En} and the $\gamma^* N \rightarrow \Delta(1232)$ quadrupole form factors data. We obtain a very good description of the G_E and G_C data when we combine the pion cloud contributions with small valence quark contributions to the $\gamma^* N \rightarrow \Delta(1232)$ quadrupole form factors. The best description of the data is obtained when the second momentum of G_{En} is $r_n^4 \simeq -0.4 \text{ fm}^4$. We conclude that the square radius associated with G_E and G_C , r_E^2 and r_C^2 , respectively, are large, revealing the long extension of the pion cloud. We conclude also that those square radius are related by $r_E^2 - r_C^2 \simeq 0.6 \text{ fm}^2$. The last result is mainly the consequence of the pion cloud effects and Siegert's theorem.

I. INTRODUCTION

From all the nucleon excitations the $\Delta(1232)$ plays a special rule, not only because it is a spin 3/2 system with the same quark content as the nucleon, but also because it is very well known experimentally [1–3]. The $\gamma^* N \rightarrow \Delta(1232)$ transition is characterized by the magnetic dipole form factor (G_M) and two quadrupole form factors: the electric (G_E) and the Coulomb (G_C) form factors [4]. The magnetic dipole is the dominate form factor, as expected from the quark spin-flip transition [5–13], but the quadrupole form factors have small but non-zero contributions [1, 2, 14–19].

Those non-zero results for the quadrupole form factors are the consequence of asymmetries on the $\Delta(1232)$ structure, which implies the deviation of the $\Delta(1232)$ from a spherical shape [2, 6, 15, 20–26]. Estimates of the electric and Coulomb quadrupole form factors based on valence quark degrees of freedom can explain in general only a small fraction of the observed data [2, 6, 7, 15, 24, 27–29]. The missing strength of the quadrupole form factors in quark models can be explained when we take into account the quark-antiquark effects or the meson cloud contributions [27, 28, 30–32].

Calculations based on $SU(6)$ quark models with symmetry breaking and large N_c limit show that in the low- Q^2 region the $\gamma^* N \rightarrow \Delta(1232)$ quadrupole form factors are dominated by pion cloud effects [2, 22, 30, 33–36]. Simple parametrizations of the pion cloud contributions to the quadrupole form factors G_E and G_C , labeled as G_E^π and G_C^π , respectively, have been derived using the

large N_c limit [30], in close agreement with the empirical data [30, 37]. Those parametrizations relate G_E^π and G_C^π with the neutron electric form factor [30, 34, 35].

There are two fundamental objections to the use of those pion cloud parametrizations: they underestimate the low- Q^2 data in about 10–20% [18, 19, 37, 38], and they are in conflict with Siegert's theorem, a fundamental constraint between the quadrupole form factors also known as the long wavelength limit [18, 19, 39–41].

Siegert's theorem states that at the pseudothreshold, when $Q^2 = Q_{pt}^2 \equiv -(M_\Delta - M)^2$, one has [4, 18, 19, 38, 42]

$$G_E(Q_{pt}^2) = \kappa G_C(Q_{pt}^2), \quad (1)$$

where M and M_Δ are the nucleon and $\Delta(1232)$ masses, respectively, and $\kappa = \frac{M_\Delta - M}{2M_\Delta}$. The pseudothreshold is the point where the photon three-momentum \mathbf{q} , vanishes ($|\mathbf{q}| = 0$), and the nucleon and the $\Delta(1232)$ are both at rest.

Concerning Siegert's theorem, the problem can be solved correcting the parametrization for G_E^π with a term $\mathcal{O}(1/N_c^2)$ at the pseudothreshold, as shown recently in Ref. [19]. Concerning the underestimation of the data associated with the quadrupole form factors G_E and G_C , it can be partially solved with the addition of contributions to those form factors associated with the valence quarks. Although small, those contributions move the estimates based on the pion cloud effects in the direction of the measured data [7, 17, 18, 28].

In the previous picture there is only a small setback, the combination of pion cloud and valence quark contributions is unable to describe previous Coulomb

quadrupole form factor data below 0.2 GeV² [18]. However, it has been shown recently that the previous extractions of G_C data at low Q^2 overestimate the actual values of the form factor [37], and that the new results are in excellent agreement with the estimates based on the pion cloud parametrizations [19].

The motivation to this work is to check if there is a parametrization of G_{En} that optimizes the description of the G_E and G_C data and provides at the same time an accurate description of the neutron electric form factor data. With this goal in mind, we perform a global fit of the functions G_{En} , G_E^π and G_C^π , to the physical form factor data, based on the pion cloud parametrization to the quadrupole form factors. An accurate description of the data indicates a correlation between the pion cloud effects in the neutron and in the $\gamma^* N \rightarrow \Delta(1232)$ transition. In addition, a global fit, which includes the G_E and G_C quadrupole form factor data can help to reduce the model dependence of the fits to G_{En} , which is a consequence of the large errorbars associated with most of the G_{En} data.

The main focus of the present work is then on the parametrization of the function G_{En} . In the past, simplified parametrizations of G_{En} with a few number of parameters have been used. Examples of those parametrizations are the Galster parametrization, the Bertozzi parametrization, based on the differences of two poles, among others [43–49]. The parametrization of G_{En} can be characterized by the first moments of the expansion of G_{En} near $Q^2 = 0$, namely, the first (r_n^2) and the second (r_n^4) moments. The explicit definitions are presented in Sec III. In the present work, motivated by a previous study of the $\gamma^* N \rightarrow \Delta(1232)$ quadrupole form factors and their relations with Siegert's theorem [18], we consider a parametrization of G_{En} based on rational functions.

As mentioned above, the description of the G_E and G_C data can be improved when we include additional contributions associated with the valence quark component. Inspired by previous works, where the valence quark contributions are estimated based on the analysis of the results from lattice QCD [9, 17, 18], we include in the present study the valence quark contributions calculated with the covariant spectator quark model from Ref. [17]. The model in discussion is covariant and consistent with the lattice QCD results [8, 17, 50]. Since in lattice QCD simulations with large pion masses the meson contributions are suppressed, the physics associated with the valence quarks can be calibrated more accurately [9]. An additional advantage in the use of a quark model framework is that the G_E and G_C form factors are identically zero at the pseudothreshold, as a consequence of the orthogonality between the nucleon and $\Delta(1232)$ states [17, 18]. This point is fundamental for the validity of Siegert's theorem.

We conclude at the end, that the combination of the G_{En} , G_E and G_C data does help to constrain the parametrization for G_{En} , although, future improvements

in the accuracy of the low- Q^2 data, for all the three form factors can further help to pin down the shape of G_{En} . The best description of the data is obtained when the second moment of G_{En} , r_n^4 is about -0.38 fm⁴. A consequence of this result is that the square radii associated with G_E and G_C (r_E^2 and r_C^2) are large, suggesting a long spacial extension of the pion cloud (or quark-antiquark distribution) for both form factors. We conclude also that, as a consequence of the pion cloud parametrizations of the G_E and G_C quadrupole form factors, one obtains $r_E^2 - r_C^2 \simeq 0.6$ fm².

This article is organized as follows: In the next section, we discuss the pion cloud parametrizations of the $\gamma^* N \rightarrow \Delta(1232)$ quadrupole form factors. In Sec. III, we discuss our parametrization of the neutron electric form factor. In Sec. IV, we present the results of the global fit to the G_{En} , G_E and G_C data, and discuss the physical consequences of the results. The outlook and conclusions are presented in Sec. V.

II. PION CLOUD PARAMETRIZATION OF G_E AND G_C

The internal structure of the baryons can be described using a combination $SU(6)$ quark models with two-body exchange currents and the large N_c limit [33–35]. The $SU(6)$ symmetry breaking induces an asymmetric distribution of charge in the nucleon and $\Delta(1232)$ systems, which is responsible for the non-vanishment of the neutron electric form factor and for the non-zero results for the $\gamma^* N \rightarrow \Delta(1232)$ quadrupole moments [35]. Those results can be derived in the context of constituent quark models as the Isgur-Karl model [51, 52], and others [2, 22, 34]. More specifically, we can conclude based on the $SU(6)$ symmetry breaking that the $\gamma^* N \rightarrow \Delta(1232)$ quadrupole moments are proportional to the neutron electric square radius (r_n^2). Based on similar arguments, we can also relate the electric quadrupole moment of the $\Delta(1232)$ and other baryons, with the neutron electric square radius [22, 23, 36, 53–55]. From the large N_c framework, we can conclude that when $Q^2 = 0$, one has $\frac{G_E}{G_M} = \mathcal{O}(\frac{1}{N_c^2})$ and $G_E = \frac{M_\Delta^2 - M^2}{4M_\Delta^2} G_C$ [2, 56].

The derivation of the pion cloud contribution to the $\gamma^* N \rightarrow \Delta(1232)$ quadrupole form factors is based on relations between the quadrupole moments and the neutron electric square radius, discussed above, and in the low- Q^2 expansion of the neutron electric form factor: $G_{En} \simeq -\frac{1}{6} r_n^2 Q^2$ [22, 30, 33–36]. One can then write

$$G_E^\pi(Q^2) = \left(\frac{M}{M_\Delta} \right)^{3/2} \frac{M_\Delta^2 - M^2}{2\sqrt{2}} \frac{\tilde{G}_{En}(Q^2)}{1 + \frac{Q^2}{2M_\Delta(M_\Delta - M)}}, \quad (2)$$

$$G_C^\pi(Q^2) = \left(\frac{M}{M_\Delta} \right)^{1/2} \sqrt{2} M_\Delta M \tilde{G}_{En}(Q^2), \quad (3)$$

where $\tilde{G}_{En} = G_{En}/Q^2$.

The previous relations are derived in Ref. [19] and improve previous large N_c relations [30], in order to satisfy Siegert's theorem exactly (1). The only difference to Ref. [30], is Eq. (2), where we include a denominator in the factor \tilde{G}_{En} . This new factor correspond to a relative correction $\mathcal{O}(1/N_c^2)$, relative to the original derivation for G_E^π , at the pseudothreshold [57]. Using the new form one obtains at the pseudothreshold: $1 + \frac{Q^2}{2M_\Delta(M_\Delta - M)} = \frac{M_\Delta + M}{2M_\Delta}$, which lead directly to Eq. (1). In a previous work [18], an approximated expression was considered for G_E^π , where the error in the description of Siegert's theorem is a term $\mathcal{O}(1/N_c^4)$.

Previous studies of Siegert's theorem based on quark models [15, 39, 58–60] show that the theorem can be violated when the operators associated with the charge density, or the current density are truncated in different orders, inducing a violation of the current conservation condition [39]. From those works we can conclude that, a consistent calculation with current conservation, requires the inclusion of processes beyond the impulse approximation at the quark level (one-body currents) and the inclusion of higher-order terms such as two-body currents, in order to be consistent with Siegert's theorem [39]. The terms with two-body currents are associated with quark-antiquark states or pion cloud contributions [38, 39]. One can then say that Eqs. (2)-(3) and their interpretation as pion/meson cloud contributions are a demand from the current conservation and an indirect consequence of Siegert's theorem.

We recall at this point that Eqs. (2)-(3) are the result of derivations valid at low Q^2 [30]. For very large values of Q^2 , we expect the pion cloud contributions to be negligible in comparison to the valence quark contributions. Thus, one can assume that for large Q^2 , Eqs. (2)-(3) are corrected according to $G_E^\pi \rightarrow G_E^\pi / (1 + Q^2 / \Lambda_E^2)^2$ and $G_C^\pi \rightarrow G_C^\pi / (1 + Q^2 / \Lambda_C^2)^4$, where Λ_E and Λ_C are large momentum cutoff parameters [19]. In those conditions the form factors G_E and G_C are, at large Q^2 , dominated by the valence quark contributions, as predicted by perturbative QCD, with falloffs $G_E \propto 1/Q^4$ and $G_C \propto 1/Q^6$ [61]. The falloff of the pion cloud components are then $G_E \propto 1/Q^8$ and $G_C \propto 1/Q^{10}$, where the extra factor $(1/Q^4)$ takes into account the effect of the extra quark-antiquark pair associated with the pion cloud [61].

Adding the valence quark contributions

The pion cloud contributions to the $\gamma^* N \rightarrow \Delta(1232)$ quadrupole form factors given by Eqs. (2)-(3) should be complemented by valence quark contributions to the respective form factors. Calculations from quarks models estimate that the valence quark contribution to the $\gamma^* N \rightarrow \Delta(1232)$ quadrupole form factors are an order of magnitude smaller than the data [1, 7, 15, 16, 62]. It is known, however, that small valence quark contributions to the quadrupole form factors can help to improve the

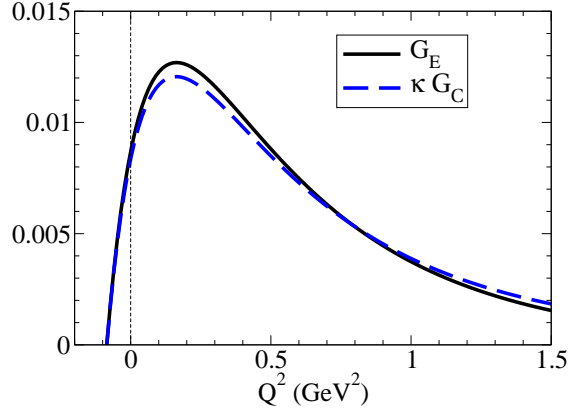


FIG. 1: Valence quark contributions for G_E and G_C according to Ref. [17]. Recall that $\kappa = \frac{M_\Delta - M}{2M_\Delta} \simeq 0.12$.

description of the data [17, 18].

The valence quark contributions to the $\gamma^* N \rightarrow \Delta(1232)$ quadrupole form factors are in general the result of high angular momentum components in the nucleon and/or $\Delta(1232)$ wave functions. The valence quark contributions to the quadrupole form factors vanish at the pseudothreshold, as a consequence of the orthogonality between the nucleon and $\Delta(1232)$ states, as discussed in Ref. [18]. In those conditions the valence quark contributions to the quadrupole form factors play no role in Siegert's theorem, which depend exclusively on the pion cloud contributions. The parameterizations (2)-(3) then ensure that Siegert's theorem is naturally satisfied.

In order to improve the description of the $\gamma^* N \rightarrow \Delta(1232)$ quadrupole form factors, we combine the pion cloud parametrizations (2)-(3) with a valence quark contributions (index B), using $G_a = G_a^B + G_a^\pi$, for $a = E, C$. For the valence quark contributions we use in particular the quark model from Ref. [17], since in this work the valence quark contributions are calculated using a extrapolation from the lattice QCD data with large pion masses [63]. Recall that in lattice QCD simulations with large pion masses, the meson cloud effects are very small, and the physics associated with the valence quarks can be better calibrated [9, 17, 64]. The model under discussion is covariant and can therefore be used to estimate the valence quark contributions in any range of Q^2 [17, 50]. The results of the valence quark contributions to the form factors G_E and G_C estimated by the model from Ref. [17] are presented in Fig. 1. The available data near $Q^2 = 0$ is $G_E(0) \simeq 0.076 \pm 0.015$ and $\kappa G_C(0.04 \text{ GeV}^2) \simeq 0.075 \pm 0.021$ [19, 37, 65]. Based on Fig. 1, one can then conclude that the valence quarks contribute only for about 10% of the empirical data near $Q^2 = 0$.

III. PARAMETRIZATIONS OF G_{En}

The parametrizations of G_{En} can be characterized by their moments, defined in the expansion near $Q^2 = 0$:

$$G_{En}(Q^2) \simeq -\frac{1}{6}r_n^2 Q^2 + \frac{1}{120}r_n^4 Q^4 + \dots, \quad (4)$$

where r_n^2 is the first moment, r_n^4 is the second moment, and so on. The first moment is well known experimentally: $r_n^2 \simeq -0.116 \text{ fm}^2$ [65]. The value of the second moment (r_n^4) controls the curvature of the function G_{En} near $Q^2 = 0$. For the second moment we need at the moment to rely on models. A discussion about possible values of r_n^4 can be found in Ref. [34].

For the following discussion it is important to introduce the most popular G_{En} parametrization, the Galster parametrization [43, 44, 47]:

$$G_{En}(Q^2) = -\frac{1}{6}r_n^2 \frac{d\tau_N}{1+d\tau_N} G_D, \quad (5)$$

where $\tau_N = \frac{Q^2}{4M^2}$, d is a free parameter, and $G_D = 1/(1+Q^2/\Lambda^2)^2$ is the nucleon dipole, with $\Lambda^2 = 0.71 \text{ GeV}^2$.

In the present work we use the following form to parametrize the function \tilde{G}_{En} :

$$\tilde{G}_{En}(Q^2) = \frac{c_0(1+c_2Q^2+\dots+c_kQ^{2k})}{1+c_1Q^2+\frac{c_1^2}{2!}Q^4+\dots+\frac{c_1^{k+3}}{(k+3)!}Q^{2k+6}}, \quad (6)$$

where $k = 2, 3, \dots$ is an integer and c_l ($l = 0, \dots, k$) are adjustable coefficients. The use of Eq. (6) is motivated by the relation between the quadrupole form factors G_E and G_C and the neutron electric form factor G_{En} , and also by previous studies of Siegert's theorem [38]. Note that for large Q^2 , one has $\tilde{G}_{En} \propto 1/Q^6$, as expected from perturbative QCD arguments [61].

The form (6) was used in Ref. [38] to parametrize the G_C data. A similar form with a different asymptotic falloff was used also for G_E ($G_E \propto 1/Q^4$, for large Q^2). From Eq. (6), one can derive the following relations for the first (r_n^2) and second (r_n^4) moments of G_{En} , as defined in Eq. (4):

$$c_0 = -\frac{1}{6}r_n^2, \quad c_0(c_2 - c_1) = \frac{1}{120}r_n^4. \quad (7)$$

We fix the value of r_n^2 by the experimental value $r_n^2 \simeq -0.116 \text{ fm}^2$ (or -2.98 GeV^{-2}), because it is determined with great accuracy. Typical values for r_n^4 are in the range $r_n^4 = -(0.60-0.30) \text{ fm}^4$ [34, 47, 48].

Because c_0 is fixed by the data, the parametrization (6) has only k independent coefficients: c_l ($l = 1, \dots, k$), meaning that there are k adjustable parameters.

IV. GLOBAL FIT

In this section we present the results of the global fit of Eqs. (2), (3) and (6) to the G_{En} , G_E and G_C data. Since

the pion cloud expressions for G_E and G_C are derived at low Q^2 [30], we restrict the fit of the quadrupole form factors to the $Q^2 < 2 \text{ GeV}^2$ region.

We start by discussing the data used in our fits and the details of those fits. Next, we present and discuss the results for G_{En} . After that we present our results to the $\gamma^* N \rightarrow \Delta(1232)$ quadrupole form factors and discuss the magnitude of the respective quadrupole square radius. At the end we debate some theoretical and experimental aspects related with the final results.

A. Data

In the present work, we consider the data for G_{En} from Refs. [49, 66]. The data from Ref. [66] are extracted from the analysis of the deuteron quadrupole form factor data, providing data at very low Q^2 . Reference [49] presents a compilation of the data from different double-polarization experiments [67-73], which measures the ratio G_{En}/G_{Mn} , where G_{Mn} is the neutron magnetic form factor.

Concerning the $\gamma^* N \rightarrow \Delta(1232)$ quadrupole form factor data, we consider a combination from the database from Ref. [74], the recent data from JLab/Hall A [37], and the world average from the Particle Data Group for $Q^2 = 0$ [65]. The database from Ref. [74] includes data from MAMI [62], MIT-Bates [75] and JLab [76] for finite Q^2 . Comparatively to Ref. [74], we replace the G_C data below 0.15 GeV^2 from Refs. [62, 75], by the new data from Ref. [37]. This procedure was adopted because it was shown that there is a discrepancy between the new data and previous measurements from MAMI and MIT-Bates [62, 75] below 0.15 GeV^2 , due to differences in the extraction procedure of the resonance amplitudes from the measured cross sections [37]. For the same reason the MAMI data from Ref. [77] are not included. As for G_E , we combine the data from Ref. [74] with the more recent data from JLab/Hall A [37].

The data for G_E and G_C are converted from the results from Refs. [37, 65, 74]. In the case of Ref. [74] the form factors G_M , G_E and G_C are calculated from the helicity amplitudes $A_{1/2}$, $A_{3/2}$ and $S_{1/2}$ using standard relations [2, 3, 40]. For the PDG [65] data at $Q^2 = 0$, we use the results from the electromagnetic ratios $R_{EM} \equiv -\frac{G_E}{G_M}$ and $R_{SM} \equiv -\frac{|\mathbf{q}|}{2M_\Delta} \frac{G_C}{G_M}$, combined with the experimental value of $G_M(0)$ [40] (\mathbf{q} is the photon three-momentum at the $\Delta(1232)$ rest frame). As for the recent data from Ref. [37] for R_{EM} and R_{SM} , we use the MAID2007 parametrization for G_M , since the helicity amplitudes are not available for all values of Q^2 . The MAID2007 parametrization for G_M can be expressed as $G_M = 3\sqrt{1+\tau}(1+a_1Q^2)e^{-a_4Q^2}$, where $\tau = \frac{Q^2}{(M_\Delta+M)^2}$, $a_1 = 0.01 \text{ GeV}^{-2}$ and $a_4 = 0.23 \text{ GeV}^{-2}$ [40], and provide a very good description of the low- Q^2 data.

In the calculation of the pion cloud contributions to G_E and G_C , we use the parametrization of G_{En} given by

c_1	c_2	c_3
3.283	-0.954	1.930

TABLE I: Parameters associated with the parametrization from Eq. (6) for the case $k = 3$.

$\chi^2(G_{En})$	$\chi^2(G_E)$	$\chi^2(G_C)$	$\chi^2(\text{tot})$
0.700	0.535	0.887	0.734

TABLE II: Quality of the parametrizations, in terms of chi-square per datapoint (G_{En} , G_E and G_C), and total chi-square per number of degrees of freedom ($\chi^2(\text{tot})$).

Eq. (6), where we take $k = 3$ (3 parameters). Comparatively to the Galster parametrization (5), we consider here an extra parameter, counting the cutoff $\Lambda^2 = 0.71$ GeV^2 as a parameter. Considering Eq. (6), we avoid an explicit dependence on the dipole factor G_D . This procedure may be more appropriated for the study of the $\gamma^* N \rightarrow \Delta(1232)$ transition form factors, since it avoids the connection with a scale associated with the nucleon [18].

Fits based on parametrizations with larger values of k ($k \geq 4$) lead to similar results at low Q^2 , but increase the number of parameters. In addition, for $k \geq 5$, the higher order coefficients c_l of the parametrizations are constrain mainly by the $Q^2 > 2$ GeV^2 data, which is restricted to 2 datapoints (2.48 GeV^2 and 3.41 GeV^2). Those coefficients are therefore poorly constraint, and can lead to strong oscillations in the function G_{En} for large Q^2 , contradicting the smooth falloff expected for large Q^2 . Parametrization of G_{En} with $k \geq 5$ may be consider, once more information relative the function G_{En} became available, such as, more and better distributed data at large Q^2 .

B. Best fit – Minimization of chi-square

The parameters associated with the best fit to the G_{En} , G_E and G_C data, defined by the minimization of chi-square, are presented in Table I, for the case $k = 3$. The quality of the combined fit can be measured by the partial values of the chi-square per datapoint. The results for the chi-square are presented in Table II. The partial results for the chi-square are presented per datapoint, because all the functions, G_{En} , G_E and G_C , depend on the same 3 parameters. Since we restrict the fit of the quadrupole form factors to $Q^2 < 2$ GeV^2 , the data for G_E and G_C is reduced to 15 and 13 datapoints, respectively. In the last column, the combined chi-square is presented per number of degrees of freedom, taking into account the number of parameters used in the global fit.

From Table II, one can conclude that we describe very well all the data subsets (G_{En} , G_E and G_C), since in

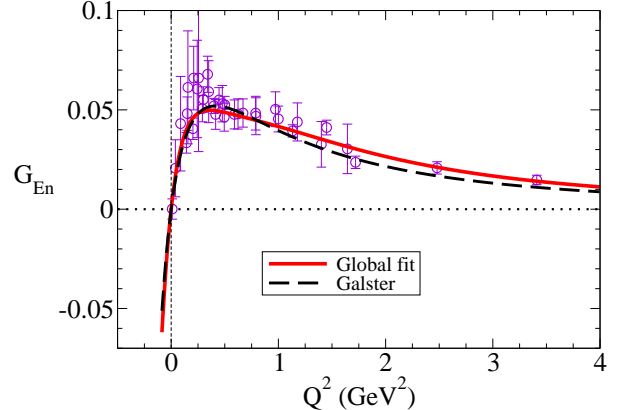


FIG. 2: Neutron electric form factor. Best fit to the data (solid-line) and Galster parametrization with $d_N = 3.02$ (dashed-line). Data from Refs. [49, 66].

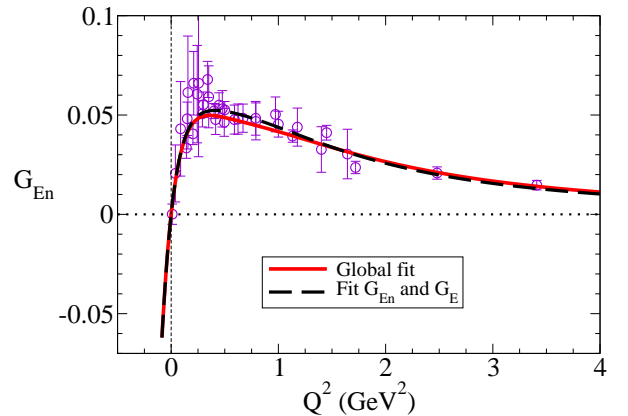


FIG. 3: Neutron electric form factor. Best fit to the data (solid-line). The dashed-line is the result of the fit that exclude the G_C data. Data from Refs. [49, 66].

all cases the chi-square per datapoint is smaller than the unit. We can also conclude that we describe also very well the combination of the 3 form factors, because the chi-square per degree of freedom is about 0.73 (smaller than the unit).

C. Neutron electric form factor (G_{En})

The numerical results for G_{En} are presented in Fig. 2 (solid-line) in comparison with the data from Refs. [49, 66]. The results for G_E and G_C are discussed later.

The quality of the description of the G_{En} data, displayed in Fig. 2 is corroborated by the value of the G_{En} partial chi-square per datapoint presented in Table II: 0.70 (smaller than the unit). In the figure, we present also the result of the Galster parametrization (5) that better describe the combination of the data, corresponding to $d_N = 3.02$ (dashed-line). It is worth to mention

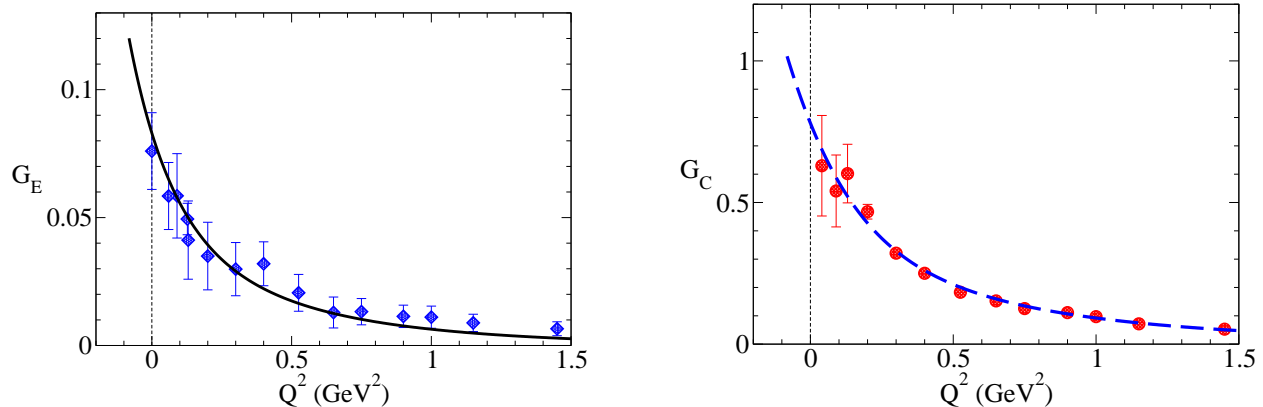


FIG. 4: $\gamma^*N \rightarrow \Delta(1232)$ electric and Coulomb quadrupole form factors. Best global fit to the data. Data from Refs. [37, 62, 65, 75, 76].

that, although consistent with the G_{En} data, this Galster parametrization is not so suitable for the description of the G_C data, as the present parametrization (solid-line). A slightly better description of the G_{En} data can be obtained with $d_N = 3.2$, but in that case the deviation from the G_C data is more significant.

In Fig. 2, we present also the results below $Q^2 = 0$ down to $Q^2 = -(M_\Delta - M)^2 \simeq -0.09 \text{ GeV}^2$, which correspond to the pseudothreshold of the $\gamma^*N \rightarrow \Delta(1232)$ transition. As mentioned, the region below $Q^2 = 0$ is important for the study of the quadrupole form factors and to Siegert's theorem [18, 19].

The parametrization presented in Fig. 2 correspond to the value

$$r_n^4 \simeq -0.383 \text{ fm}^4. \quad (8)$$

This estimate is close to other estimates presented in the literature based on the Galster parametrization [34] and also other parametrizations [48]. For the propose of the discussion, we note that a Galster parametrization that provides a good description of the G_{En} data, associated with $d_N = 2.8$ [18, 19, 33] correspond to $r_n^4 \simeq -0.30 \text{ fm}^4$.

It is also worth mentioning that in a parametrization that include the factor G_D , a significant contribution to r_n^4 comes from a term on $1/\Lambda^2$, where $\Lambda^2 = 0.71 \text{ GeV}^2$. In a Galster parametrization, the last contribution is about -0.25 fm^4 . It is then interesting to conclude that we obtain a result close to the Galster parametrizations, without including the factor G_D .

In order to test the dependence of the fit on the data subsets, we performed also partial fits to the combination of the data (G_{En}, G_E) and (G_{En}, G_C). This way, we can test which quadrupole set, G_E or G_C , has more impact in the global fit, and also infer if those sets are compatible with the G_{En} data. The result of the combined fit for (G_{En}, G_C) is almost undistinguished from the global fit (solid-line), and it is not presented for clarity. The result of the fit to the sets (G_{En}, G_C) is represented in Fig. 3 by the dashed-line. From the difference between the two

lines we can conclude that the G_E and G_C data are compatible with some deviations from the relations (2) and (3), respectively. However, we can also conclude that the magnitude of the deviation is small. Note in particular that both lines have the almost same shape for $Q^2 < 0.1 \text{ GeV}^2$.

Concerning the possibility of a small bump in the function G_{En} near $Q^2 = 0.2\text{--}0.3 \text{ GeV}^2$, discussed extensively in the literature [30, 45], we conclude that the present accuracy of the data is insufficient for more definitive conclusions. Our best fit has a smooth behavior in the region under discussion. Nevertheless, larger values of k can in principle generate a low- Q^2 bump, once one has more high Q^2 data to constrain the higher order coefficients.

D. Quadrupole form factors (G_E, G_C)

The results for the best global fit to the $\gamma^*N \rightarrow \Delta(1232)$ quadrupole form factors are presented in Fig. 4, in comparison with the respective data. In the figure, we can observe an excellent agreement with the data in the range $Q^2 = 0\text{--}1.5 \text{ GeV}^2$, for both form factors. The quality of the description is also corroborated by the partial chi-square per datapoint presented in Table II, which is 0.54 and 0.89, for G_E and G_C , respectively. For this agreement contributes the larger errorbars for the data below 0.2 GeV^2 . The precision of the $Q^2 < 0.2 \text{ GeV}^2$ data is comparable with the precision of most of the neutron electric form factor data. The agreement with the data and the magnitude of the errorbars can be observed in the graphs.

In Fig. 5, we compare the results for G_E with the results for G_C corrected by the factor κ . In this representation it is more explicit the connection between the two quadrupole form factors and the implication of Siegert's theorem. The convergence of the results at the pseudothreshold ($Q^2 \simeq -0.09 \text{ GeV}^2$), consequence

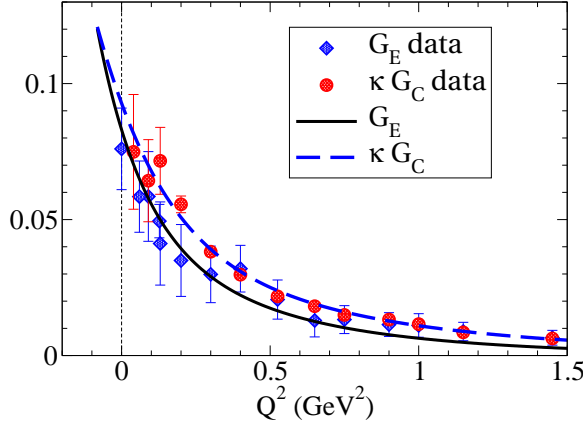


FIG. 5: Results for the form factors G_E and G_C . Data from Refs. [37, 62, 65, 75, 76]. Recall that $\kappa = \frac{M_\Delta - M}{2M_\Delta} \simeq 0.12$.

of Siegert's theorem, is clearly displayed in the graph.

In comparison with the results from Ref. [19], where G_{En} is described by a Galster parametrization ($d_n = 2.8$), we obtain slightly larger values for the quadrupole form factors at the pseudothreshold.

Based on the results of G_E and G_C at $Q^2 = 0$, one can test the accuracy of the large N_c estimate $G_E = \frac{M_\Delta^2 - M^2}{4M_\Delta^2} G_C$, apart $\mathcal{O}(\frac{1}{N_c^2})$ relative corrections [30]. According to the results from Fig. 5, one obtain $G_E(0) \simeq 0.0830$ and $\frac{M_\Delta^2 - M^2}{4M_\Delta^2} G_C(0) \simeq 0.0818$, in close agreement with the large N_c prediction (1.5% deviation). The previous relation is equivalent to the identity $R_{EM}(0) = R_{SM}(0)$ [19, 30].

E. Square radius r_E^2 and r_C^2

The difference of behavior between the two form factors can be better understood when we look at the square radius associated with the quadrupole form factors G_E and G_C , defined by [35, 38, 78]

$$r_a^2 = -\frac{14}{G_a(0)} \left. \frac{dG_a}{dQ^2} \right|_{Q^2=0} \quad (9)$$

where $a = E, C$. The numerical results for r_E^2 and r_C^2 for the parametrizations discussed here are presented in Table III.

If we ignore the effect of the valence quarks, one can calculate r_E^2 and r_C^2 very easily using Eqs. (2)-(3). One obtains then $r_E^2 = \frac{7}{10} \frac{r_n^4}{r_n^2} + \frac{7}{M_\Delta(M_\Delta - M)}$ and $r_C^2 = \frac{7}{10} \frac{r_n^4}{r_n^2}$. The relation for r_C^2 was derived previously in Ref. [35], assuming the dominance of the pion cloud contribution. Using the result (8) for r_n^4 , one obtains the estimates $r_E^2 \simeq 3.06 \text{ fm}^2$ and $r_C^2 \simeq 2.31 \text{ fm}^2$. Both estimates are about 10% larger than the results for the pion cloud contribution presented in Table III. Those estimates are con-

	r_E^2 (fm 2)	r_C^2 (fm 2)	$r_E^2 - r_C^2$ (fm 2)
B	-0.410	-0.347	-0.063
π	2.742	2.100	0.643
Total	2.331	1.752	0.580

TABLE III: Contributions to the quadrupole square radius (bare and pion cloud): r_E^2 , r_C^2 and difference $r_E^2 - r_C^2$.

sistent with the 10% correction, discussed earlier, associated with the inclusion of the valence quark contributions for both the quadrupole form factors, near $Q^2 = 0$.

Combining the analytic expressions described previously for r_E^2 and r_C^2 , one has $r_E^2 - r_C^2 = \frac{7}{M_\Delta(M_\Delta - M)} \simeq 0.75 \text{ fm}^2$. Note that this result is independent of the general form used for the function G_{En} , and therefore independent of r_n^4 .

The previous estimate differs from the result presented in Table III, mostly because of the valence quark effects are not taken into account as discussed above (10% reduction). Correcting the previous result with the valence quark effect, assuming the 10% correction, one obtain then $(r_E^2 - r_C^2)_\pi \simeq 0.68 \text{ fm}^2$. The subindex was included to emphasize that the estimate concerns the pion cloud component. The previous estimate is still in disagreement with the result from Table III, in about -0.04 fm^2 .

To understand the previous difference, we need to look into the details of the calculation, and for the very small deviations from the 10% correction, assumed for the valence quark component. If we consider deviation of δ_E and δ_C from the 10% correction to the form factors G_E and G_C , respectively, we conclude that the residual correction can be expressed as $0.9^2(\delta_C - \delta_E)r_{E0}^2$, where the first factor accounts for the 10% correction in the normalizations, and r_{E0}^2 is the estimate of r_E^2 in a model with pion cloud dominance, mentioned above. Combining all effects with $r_{E0}^2 \simeq 3.06 \text{ fm}^2$, one obtain $0.9^2(\delta_C - \delta_E)r_{E0}^2 \simeq -0.04 \text{ fm}^2$, which explain at last the result $(r_E^2 - r_C^2)_\pi \simeq 0.64 \text{ fm}^2$. The last correction is then the consequence of product of a very small factor with a large factor (r_{E0}^2).

The contributions from the valence quark component depend on the details of the quark model, and are therefore model dependent. Using the model described previously we obtain $(r_E^2 - r_C^2)_B \simeq -0.06 \text{ fm}^2$, where B labels the bare contribution. Combining the two contributions, we obtain $r_E^2 - r_C^2 \simeq 0.58 \text{ fm}^2$, as presented in Table III.

Smaller values for r_C^2 have been suggested by empirical parametrizations of the quadrupole form factor data consistent with Siegert's theorem [18, 38]. We note, however, that those estimates are strongly affected by the $Q^2 = 0-0.15 \text{ GeV}^2$ data for G_C , from Refs. [62, 75, 77]. Therefore, the conclusions based on those data have to be reviewed in light of the new data from Ref. [37].

An important conclusion from the previous discussion is that the in order to obtain a reliable estimate of r_E^2 and

r_C^2 from the G_E and G_C data, we need more accurate measurements from G_E and G_C near $Q^2 = 0$.

Overall, we can conclude that the large values obtained for r_E^2 and r_C^2 are the outcome of the pion cloud dominance. The magnitudes of r_E^2 and r_C^2 around 2 fm^2 can be interpreted physically, as the result of the increment of the size of the constituent quarks due to the $q\bar{q}$ pair/pion cloud dressing [35, 38]. More specifically, those magnitudes can be understood looking at the pion Compton scattering wavelength, $r_\pi \approx 1/m_\pi$, which characterize the pion distribution inside the nucleon [35]. Numerically, the result $r_E^2 \approx r_C^2 \approx 2 \text{ fm}^2$ is then the consequence of $r_E^2 \approx r_C^2 \approx r_\pi^2$. A more detailed discussion on this subject can be found in Ref. [35].

Concerning the difference $r_E^2 - r_C^2 \simeq 0.6 \text{ fm}^2$, one can conclude that it is mainly a consequence of Siegert's theorem, since the difference between r_E^2 and r_C^2 is the consequence of the extra factor included in the pion cloud parametrization G_E^π , in order to satisfy Siegert's theorem.

F. General discussion

Once presented our final results for the neutron electric form factor and for $\gamma^* N \rightarrow \Delta(1232)$ quadrupole form factors, one can discuss some theoretical and experimental aspects related to the present results.

It is important to emphasize that for the excellent agreement between model and the data for the quadrupole form factors, displayed in Figs. 4 and 5, contributes also the valence quark contributions estimated with a covariant quark model. We stress that this part of the calculation is model dependent. A test to the valence quark contributions can be performed in a near future with lattice QCD simulations in the range of $m_\pi = 0.2 - 0.3 \text{ GeV}$ [81], a region close to the physical point, but where hopefully the pion cloud contamination is small.

Another relevant point of discussion is the accuracy of the data. The data associate with G_{En} have in general large errorbars, which difficult the derivation of an accurate parametrization. The G_E and G_C data below 0.15 GeV^2 are also affected by large errorbars. For those reasons it is not hard to find parametrizations that provide a good description of the overall data including the low- Q^2 region (small chi-square). The inclusion of the G_E and G_C data provide, however, additional constraints to the function G_{En} , which can help to improve the description of the neutron electric form factor.

Another important aspect in the present work is the sensitivity of the fits to the data, particularly in the region $Q^2 = 0 - 0.2 \text{ GeV}^2$. This effect can be illustrated by the realization that the trend of the function G_C changed with the more recent data [37]. A fit that includes the G_C data from Refs. [62, 75] cannot describe the data with the same accuracy as a fit that include the more recent data [18]. In conclusion, the new data for G_C have also a significant impact in the solution for G_{En} .

To finish the present discussion, we note that additional tests for the results of the functions G_E and G_C can be performed using lattice QCD simulations not too far away from the physical point. Combining lattice QCD results with expansions on the pion mass, derived from effective field theories [79, 80], one can test the consistency between the results from lattice and the experimental data, and therefore, the consistency between QCD and the real world.

V. OUTLOOK AND CONCLUSIONS

In the present work, we derive a global parametrization of the neutron electric form factor and the $\gamma^* N \rightarrow \Delta(1232)$ quadrupole form factors, G_E and G_C . To relate the pion cloud contribution to G_E and G_C with the neutron electric form factor we use improved relations derived in the large N_c limit in order to verify Siegert's theorem exactly.

The success of the global parametrization of G_{En} , G_E and G_C is an indication of the importance of the pion cloud in the neutron and in the $\gamma^* N \rightarrow \Delta(1232)$ transition. This correlation is suggested by the large N_c limit, by the $SU(6)$ symmetry breaking, and by calculations based on constituent quark models.

To the agreement between the model calculations and the empirical data for the $\gamma^* N \rightarrow \Delta(1232)$ quadrupole form factors also contributes small valence quark components estimated by a covariant quark model, calibrated previously with lattice QCD data.

The global fit of the G_{En} , G_E and G_C data, based on rational functions, show that the overall data, and the G_{En} data in particular, is compatible with a smooth description of the neutron electric form factor, with no pronounced bump at low Q^2 . The best description of the data is obtained when we consider a parametrization of G_{En} associated with $r_n^4 \simeq -0.4 \text{ fm}^4$.

We conclude that the square radius associated with the quadrupole form factors G_E and G_C are large, as a consequence of the pion cloud effects (long extension of the pion cloud). We conclude also that the square radius, r_E^2 and r_C^2 are constrain by the relation $r_E^2 - r_C^2 \simeq 0.6 \text{ fm}^2$. The previous relation is a consequence of Siegert's theorem and of the dominance of the pion cloud contributions on the quadrupole form factors G_E and G_C .

The present parametrization of the neutron electric form factor is still derived from data with significant errorbars below 0.2 GeV^2 . Future experiments with more accurate data for G_{En} , and the $\gamma^* N \rightarrow \Delta(1232)$ quadrupole form factors can help to elucidate the shape of the function G_{En} at low Q^2 .

Acknowledgments

The author thanks Mauro Giannini for helpful discussions. This work was supported by the Fundação de Amparo à Pesquisa do Estado de São Paulo (FAPESP): project no. 2017/02684-5, grant no. 2017/17020-BCO-JP.

[1] I. G. Aznauryan *et al.*, Int. J. Mod. Phys. E **22**, 1330015 (2013) [arXiv:1212.4891 [nucl-th]].

[2] V. Pascalutsa, M. Vanderhaeghen and S. N. Yang, Phys. Rept. **437**, 125 (2007) [hep-ph/0609004].

[3] I. G. Aznauryan and V. D. Burkert, Prog. Part. Nucl. Phys. **67**, 1 (2012) [arXiv:1109.1720 [hep-ph]].

[4] H. F. Jones and M. D. Scadron, Annals Phys. **81**, 1 (1973).

[5] M. A. B. Beg, B. W. Lee and A. Pais, Phys. Rev. Lett. **13**, 514 (1964).

[6] C. Becchi and G. Morpurgo, Phys. Lett. **17**, 352 (1965).

[7] B. Julia-Diaz, T.-S. H. Lee, T. Sato and L. C. Smith, Phys. Rev. C **75**, 015205 (2007) [nucl-th/0611033].

[8] G. Ramalho, M. T. Peña and F. Gross, Eur. Phys. J. A **36**, 329 (2008) [arXiv:0803.3034 [hep-ph]].

[9] G. Ramalho and M. T. Peña, J. Phys. G **36**, 115011 (2009) [arXiv:0812.0187 [hep-ph]].

[10] G. Ramalho and K. Tsushima, Phys. Rev. D **87**, 093011 (2013) [arXiv:1302.6889 [hep-ph]]; G. Ramalho and K. Tsushima, Phys. Rev. D **88**, 053002 (2013) [arXiv:1307.6840 [hep-ph]].

[11] G. Eichmann and D. Nicmorus, Phys. Rev. D **85**, 093004 (2012) [arXiv:1112.2232 [hep-ph]].

[12] J. Segovia, C. Chen, C. D. Roberts and S. Wan, Phys. Rev. C **88**, 032201 (2013) [arXiv:1305.0292 [nucl-th]].

[13] H. Sanchis-Alepuz, R. Alkofer and C. S. Fischer, arXiv:1707.08463 [hep-ph].

[14] N. Isgur, G. Karl and R. Koniuk, Phys. Rev. D **25**, 2394 (1982).

[15] S. Capstick and G. Karl, Phys. Rev. D **41**, 2767 (1990).

[16] G. Ramalho, M. T. Peña and F. Gross, Phys. Rev. D **78**, 114017 (2008) [arXiv:0810.4126 [hep-ph]].

[17] G. Ramalho and M. T. Peña, Phys. Rev. D **80**, 013008 (2009) [arXiv:0901.4310 [hep-ph]].

[18] G. Ramalho, Phys. Rev. D **94**, 114001 (2016) [arXiv:1606.03042 [hep-ph]].

[19] G. Ramalho, arXiv:1709.07412 [hep-ph].

[20] S. L. Glashow, Physica A **96**, 27 (1979).

[21] A. M. Bernstein, Eur. Phys. J. A **17**, 349 (2003) [hep-ex/0212032].

[22] A. J. Buchmann, E. Hernandez and A. Faessler, Phys. Rev. C **55**, 448 (1997) [nucl-th/9610040].

[23] M. I. Krivoruchenko and M. M. Giannini, Phys. Rev. D **43**, 3763 (1991).

[24] A. J. Buchmann and E. M. Henley, Phys. Rev. C **63**, 015202 (2000) [arXiv:hep-ph/0101027].

[25] G. Ramalho, M. T. Peña and A. Stadler, Phys. Rev. D **86**, 093022 (2012) [arXiv:1207.4392 [nucl-th]].

[26] G. Ramalho, M. T. Peña and F. Gross, Phys. Lett. B **678**, 355 (2009) [arXiv:0902.4212 [hep-ph]]. G. Ramalho, M. T. Peña and F. Gross, Phys. Rev. D **81**, 113011 (2010) [arXiv:1002.4170 [hep-ph]].

[27] L. Tiator, D. Drechsel, S. Kamalov, M. M. Giannini, E. Santopinto and A. Vassallo, Eur. Phys. J. A **19**, 55 (2004) [nucl-th/0310041].

[28] S. S. Kamalov and S. N. Yang, Phys. Rev. Lett. **83**, 4494 (1999) [nucl-th/9904072]; S. S. Kamalov, S. N. Yang, D. Drechsel, O. Hanstein and L. Tiator, Phys. Rev. C **64**, 032201 (2001) [nucl-th/0006068].

[29] T. Sato and T. S. H. Lee, Phys. Rev. C **63**, 055201 (2001) [nucl-th/0010025].

[30] V. Pascalutsa and M. Vanderhaeghen, Phys. Rev. D **76**, 111501 (2007) [arXiv:0711.0147 [hep-ph]].

[31] M. Fiolhais, B. Golli and S. Širca, Phys. Lett. B **373**, 229 (1996).

[32] D. H. Lu, A. W. Thomas and A. G. Williams, Phys. Rev. C **55**, 3108 (1997).

[33] A. J. Buchmann, Phys. Rev. Lett. **93**, 212301 (2004) [hep-ph/0412421].

[34] P. Grabmayr and A. J. Buchmann, Phys. Rev. Lett. **86**, 2237 (2001) [hep-ph/0104203].

[35] A. J. Buchmann, Can. J. Phys. **87**, 773 (2009) [arXiv:0910.4747 [physics.atom-ph]].

[36] A. J. Buchmann, J. A. Hester and R. F. Lebed, Phys. Rev. D **66**, 056002 (2002) [hep-ph/0205108].

[37] A. Blomberg *et al.*, Phys. Lett. B **760**, 267 (2016) [arXiv:1509.00780 [nucl-ex]].

[38] G. Ramalho, Phys. Rev. D **93**, 113012 (2016) [arXiv:1602.03832 [hep-ph]].

[39] A. J. Buchmann, E. Hernandez, U. Meyer and A. Faessler, Phys. Rev. C **58**, 2478 (1998).

[40] D. Drechsel, S. S. Kamalov and L. Tiator, Eur. Phys. J. A **34**, 69 (2007) [arXiv:0710.0306 [nucl-th]].

[41] L. Tiator and S. Kamalov, AIP Conf. Proc. **904**, 191 (2007) [nucl-th/0610113]; L. Tiator, Few Body Syst. **57**, 1087 (2016).

[42] G. Ramalho, Phys. Lett. B **759**, 126 (2016) [arXiv:1602.03444 [hep-ph]].

[43] S. Galster, H. Klein, J. Moritz, K. H. Schmidt, D. Wegener and J. Bleckwenn, Nucl. Phys. B **32**, 221 (1971).

[44] J. J. Kelly, Phys. Rev. C **66**, 065203 (2002) [hep-ph/0204239].

[45] J. Friedrich and T. Walcher, Eur. Phys. J. A **17**, 607 (2003) [hep-ph/0303054].

[46] W. Bertozi, J. Friar, J. Heisenberg and J. W. Negele, Phys. Lett. **41B**, 408 (1972).

[47] S. Platchkov *et al.*, Nucl. Phys. A **510**, 740 (1990).

[48] M. M. Kaskulov and P. Grabmayr, Eur. Phys. J. A **19**, 157 (2004) [nucl-th/0308015].

[49] T. R. Gentile and C. B. Crawford, Phys. Rev. C **83**, 055203 (2011).

[50] F. Gross, G. Ramalho and M. T. Peña, Phys. Rev. C **77**, 015202 (2008) [nucl-th/0606029].

[51] N. Isgur, G. Karl and D. W. L. Sprung, Phys. Rev. D **23**, 163 (1981).

[52] N. Isgur and G. Karl, Phys. Rev. D **19**, 2653 (1979) Erratum: [Phys. Rev. D **23**, 817 (1981)]; N. Isgur and G. Karl, Phys. Rev. D **20**, 1191 (1979).

[53] G. Dillon and G. Morpurgo, Phys. Lett. B **448**, 107 (1999).

[54] A. J. Buchmann and E. M. Henley, Phys. Rev. D **65**, 073017 (2002).

[55] A. J. Buchmann and R. F. Lebed, Phys. Rev. D **62**, 096005 (2000) [hep-ph/0003167].

[56] E. E. Jenkins, X. Ji and A. V. Manohar, Phys. Rev. Lett. **89**, 242001 (2002) [hep-ph/0207092].

[57] Since in the large N_c limit $M_\Delta - M = \mathcal{O}(1/N_c)$, and $M_\Delta = \mathcal{O}(N_c)$, the factor $1/\left(1 + \frac{Q^2}{(M_\Delta + M)^2}\right)$, correspond to a correction $\mathcal{O}(1/N_c^2)$, at the pseudothreshold.

[58] D. Drechsel and M. M. Giannini, Phys. Lett. **143B**, 329 (1984).

[59] M. Weyrauch and H. J. Weber, Phys. Lett. B **171**, 13 (1986) [Phys. Lett. B **181**, 415 (1986)].

[60] M. Bourdeau and N. C. Mukhopadhyay, Phys. Rev. Lett. **58**, 976 (1987).

[61] C. E. Carlson and N. C. Mukhopadhyay, Phys. Rev. Lett. **81**, 2646 (1998) [hep-ph/9804356]; C. E. Carlson, Phys. Rev. D **34**, 2704 (1986).

[62] S. Stave *et al.* [A1 Collaboration], Phys. Rev. C **78**, 025209 (2008) [arXiv:0803.2476 [hep-ex]].

[63] C. Alexandrou, G. Koutsou, H. Neff, J. W. Negele, W. Schroers and A. Tsapalis, Phys. Rev. D **77**, 085012 (2008) [arXiv:0710.4621 [hep-lat]].

[64] G. Ramalho, K. Tsushima and F. Gross, Phys. Rev. D **80**, 033004 (2009) [arXiv:0907.1060 [hep-ph]].

[65] K. A. Olive *et al.* [Particle Data Group Collaboration], Chin. Phys. C **38**, 090001 (2014).

[66] R. Schiavilla and I. Sick, Phys. Rev. C **64**, 041002 (2001) [arXiv:nucl-ex/0107004].

[67] T. Eden *et al.*, Phys. Rev. C **50**, 1749 (1994).

[68] I. Passchier *et al.*, Phys. Rev. Lett. **82**, 4988 (1999) [arXiv:nucl-ex/9907012].

[69] C. Herberg *et al.*, Eur. Phys. J. A **5**, 131 (1999); D. I. Glazier *et al.*, Eur. Phys. J. A **24**, 101 (2005) [arXiv:nucl-ex/0410026].

[70] J. Bermuth *et al.*, Phys. Lett. B **564**, 199 (2003) [nucl-ex/0303015].

[71] H. Zhu *et al.* [E93026 Collaboration], Phys. Rev. Lett. **87**, 081801 (2001) [arXiv:nucl-ex/0105001]; R. Madey *et al.* [E93-038 Collaboration], Phys. Rev. Lett. **91**, 122002 (2003) [arXiv:nucl-ex/0308007]; G. Warren *et al.* [Jefferson Lab E93-026 Collaboration], Phys. Rev. Lett. **92**, 042301 (2004) [arXiv:nucl-ex/0308021].

[72] E. Geis *et al.* [BLAST Collaboration], Phys. Rev. Lett. **101**, 042501 (2008) [arXiv:0803.3827 [nucl-ex]].

[73] S. Riordan *et al.*, Phys. Rev. Lett. **105**, 262302 (2010) [arXiv:1008.1738 [nucl-ex]].

[74] V. I. Mokeev, https://userweb.jlab.org/~mokeev/resonance_electrocouplings/

[75] N. F. Sparveris *et al.* [OOPS Collaboration], Phys. Rev. Lett. **94**, 022003 (2005) [nucl-ex/0408003].

[76] J. J. Kelly *et al.*, Phys. Rev. C **75**, 025201 (2007) [nucl-ex/0509004]; I. G. Aznauryan *et al.* [CLAS Collaboration], Phys. Rev. C **80**, 055203 (2009) [arXiv:0909.2349 [nucl-ex]].

[77] N. Sparveris *et al.*, Eur. Phys. J. A **49**, 136 (2013) [arXiv:1307.0751 [nucl-ex]].

[78] T. De Forest, Jr. and J. D. Walecka, Adv. Phys. **15**, 1 (1966).

[79] V. Pascalutsa and M. Vanderhaeghen, Phys. Rev. Lett. **95**, 232001 (2005) [hep-ph/0508060].

[80] T. A. Gail and T. R. Hemmert, Eur. Phys. J. A **28**, 91 (2006) [nucl-th/0512082].

[81] C. Alexandrou, G. Koutsou, J. W. Negele, Y. Proestos and A. Tsapalis, Phys. Rev. D **83**, 014501 (2011) [arXiv:1011.3233 [hep-lat]].